Applied Magnetic Resonance (2022) 53:653–669
https://doi.org/10.1007/s00723-021-01377-4

Applied
Magnetic Resonance

ORIGINAL PAPER

Gas-Phase NMR of Hyperpolarized Propane with ^{1}H-to-^{13}C Polarization Transfer by PH-INEPT

Dudari B. Burueva[1,2] · Vitaly P. Kozinenko[1,2] · Sergey V. Sviyazov[1,2] · Larisa M. Kovtunova[1,3] · Valerii I. Bukhtiyarov[2,3] · Eduard Y. Chekmenev[4,5] · Oleg G. Salnikov[1,2,3] · Kirill V. Kovtunov[1,2] · Igor V. Koptyug[1]

Received: 28 April 2021 / Revised: 16 June 2021 / Accepted: 20 June 2021 /
Published online: 14 July 2021

Abstract

In this work we demonstrate the possibility to transfer parahydrogen-derived ^{1}H polarization to ^{13}C nuclei in the gas phase using PH-INEPT-based pulse sequences. The propane with hyperpolarized ^{1}H nuclei was produced via hydrogenation of propylene (at natural ^{13}C abundance) with parahydrogen over the heterogeneous 1 wt% Rh/TiO_2 catalyst at 7.05 T magnetic field of a NMR spectrometer. The apparent proton polarization was estimated as $1.8 \pm 0.4\%$, taking into account the polarization losses caused by spin relaxation. The optimal inter-pulse delays for both the PH-INEPT and the PH-INEPT + sequences were determined via the numerical calculations considering the full spin system of propane which includes eight protons and one ^{13}C nucleus. The application of the optimized PH-INEPT polarization transfer sequence resulted in the ^{13}C polarization values of $0.07 \pm 0.01\%$ and $0.030 \pm 0.006\%$ for the methyl group of [1-^{13}C]propane and the methylene group of [2-^{13}C]propane, respectively. The experimental dependence of the ^{13}C polarization values for [1-^{13}C]propane and [2-^{13}C]propane on the inter-pulse delay τ_1 of the PH-INEPT sequence is in a good agreement with the simulation. The resulting ^{13}C polarization using PH-INEPT + sequence is ~ 2.5 times lower than that via PH-INEPT, which is also consistent with the numerical calculations.

Kirill V. Kovtunov: Deceased.

✉ Igor V. Koptyug
koptyug@tomo.nsc.ru

1 International Tomography Center SB RAS, 3A Institutskaya St., Novosibirsk 630090, Russia

2 Novosibirsk State University, 2 Pirogova St., Novosibirsk 630090, Russia

3 Boreskov Institute of Catalysis SB RAS, 5 Acad. Lavrentiev Ave., Novosibirsk 630090, Russia

4 Wayne State University, 5101 Cass Ave, Detroit, MI 48202, USA

5 Russian Academy of Sciences, 14 Leninskiy Prospekt, Moscow 119991, Russia

1 Introduction

One of the most promising and robust hyperpolarization (HP) techniques aiming to increase sensitivity in NMR and MRI experiments is parahydrogen-induced nuclear polarization (PHIP) [1]. It relies on the conversion of the singlet order of parahydrogen (p-H_2, the spin isomer of molecular hydrogen with a total nuclear spin $I=0$) into observable NMR signals, which can be enhanced by several orders of magnitude. In canonical PHIP, signal enhancement is achieved via p-H_2 pairwise addition to an unsaturated substrate during catalytic hydrogenation [2, 3]. To preserve the spin correlation of p-H_2-derived protons upon their incorporation into a product molecule, hydrogenation must proceed via pairwise H_2 addition, and p-H_2-derived protons must end up in magnetically inequivalent positions in order for the enhancement of the NMR signals to be observed. In theory, proton polarization achieved by PHIP can approach 100%, meaning that NMR signal enhancement values of up to 10^4–10^5 are possible in high-field NMR [4]. The PHIP effect was first demonstrated by Bowers and Weitekamp in a homogeneous hydrogenation of acrylonitrile over Wilkinson's catalyst, the catalytic cycle of which is known to proceed via pairwise addition of H_2 [2]. In contrast, it was believed that PHIP effects cannot be observed using solid heterogeneous catalysts, which activate H_2 molecule in a dissociative manner and should lead to a rapid loss of spin correlation between p-H_2-derived chemisorbed hydrogen atoms [5]. However, despite this commonly accepted wisdom, PHIP effects were successfully demonstrated in a heterogeneous hydrogenation over Wilkinson's catalyst immobilized on a solid support [6] and shortly after over Pt metal catalyst supported on alumina [7]. The latter research gave rise to a vast majority of works in the field of PHIP in heterogeneous hydrogenations (HET-PHIP). As hyperpolarization in PHIP is created in a chemical reaction, the HET-PHIP technique allows one to study heterogeneous catalytic reactions [8]. Due to a significant NMR signal enhancement, detection of short-lived intermediates of catalytic reactions becomes possible in principle, which has a potential to greatly advance understanding of the mechanisms of these reactions. Applications of HET-PHIP in catalysis are covered in the most recent reviews [8, 9], but the utility of HET-PHIP is not limited to the studies of catalytic processes. An important advantage of HET-PHIP is the possibility to produce catalyst-free hyperpolarized fluids for biomedical MRI, since heterogeneous catalysts can be easily separated from a hyperpolarized product. In this context, HP propane, which can be potentially used as a safe and inexpensive contrast agent [10] for in vivo lung MRI, is of particular interest [11, 12]. The possibility of producing HP propane on a clinical scale in the heterogeneous hydrogenation of propylene with parahydrogen over Rh/TiO_2 catalyst was recently demonstrated [13]. HP propane was also produced in the hydrogenation of cyclopropane [14, 15]. The use of cyclopropane as a substrate instead of propylene for propane production seems promising—the resulting propane has surprisingly high polarization levels, and an incomplete conversion is not an issue, since the remaining cyclopropane is nontoxic. Besides, the possibility to use diethyl ether as a promising HP contrast agent has recently been

demonstrated [16]. Diethyl ether is attractive as a contrast agent because it was used for a long time in anesthesia, which should accelerate clinical translation. Moreover, the ethyl vinyl ether precursor, which was hydrogenated to yield diethyl ether, is also used as an anesthetic.

One of the most promising strategies for PHIP applications is the transfer of proton hyperpolarization to magnetic heteronuclei, namely, ^{13}C, ^{15}N, and others [17]. These nuclei exhibit such unique features as long relaxation times (typically, in liquid phase) and background-free detection, which makes them ideal sensors for biomedical NMR and MRI applications [18, 19]. However, detection of such nuclei is rather difficult, which is the result of small values of their magnetic moments and a low natural abundance. Fortunately, transferring the proton polarization supplied by PHIP to heteronuclei provides an effective remedy for this problem. It can be performed via different approaches—by magnetic field cycling [20–27] and by radiofrequency (rf) pulse sequences [28–36]. However, to the best of our knowledge, neither approach was applied to gases so far. Here in this work, we demonstrate ^{1}H-to-^{13}C polarization transfer for propane isotopomers at natural isotopic abundance in the gas phase using PH-INEPT pulse sequence [33]. Since the gas molecules constitute a well-defined uniform physical system, ^{13}C HP gases can be advantageous for studying fundamental intramolecular and intermolecular interactions and the mechanisms of nuclear spin relaxation using ^{13}C NMR spectroscopy [37, 38].

Hyperpolarized propane was produced via HET-PHIP using a heterogeneous Rh/TiO_2 catalyst under PASADENA conditions and the ^{1}H polarization was subsequently transferred to ^{13}C nuclei. In the case of a gas-phase process implemented under continuous flow conditions, rapid relaxation of spins and escape of HP molecules from the detection zone forced us to seek the fastest way to transfer polarization. Among the variety of polarization transfer techniques, PH-INEPT-based transfer is the best option for the case of weakly coupled p-H_2-derived protons, which is the case for propane molecule in the high magnetic field of an NMR spectrometer. The total time of transfer is determined by the J-coupling between the p-H_2 derived protons and a heteronucleus, and for propane molecule possessing a ^{13}C nucleus it is on the order of tens of milliseconds. The rf-based polarization transfer occurs directly in the NMR signal detection zone, which reduces polarization losses during the time between the formation of HP molecules and their NMR detection. PH-INEPT-based transfer utilizes hard rf pulses, making it non-selective with respect to the chemical shifts of heteronuclei in the molecules under study.

2 Experimental Section

2.1 Catalyst Preparation and Characterization

The Rh/TiO_2 catalyst used in this work was prepared by wet impregnation of titanium dioxide with a rhodium nitrate solution [39]. Titanium dioxide TiO_2 (HombifineN, 100% anatase, BET specific surface area $S_{BET} = 360$ m^2 g^{-1}) was calcined at 550 °C for 2 h, which resulted in a decrease of S_{BET} to 109 m^2 g^{-1}. The required amount of rhodium(III) nitrate hydrate (Sigma Aldrich, 83750; Rh content ~ 36 wt%)

was dissolved in distilled water, and this aqueous solution was used to impregnate titanium dioxide for 1 h at room temperature. Solvent excess was evaporated at a reduced pressure. The sample was dried at 120 °C for 3 h and then calcined at 400 °C for 4 h followed by reduction in H_2 flow (75 cm^3 min^{-1}, 1 atm) at 330 °C for 3 h. The catalyst contained ~ 1% Rh by weight.

2.2 Hydrogenation Experiments

Propylene (purity > 99.6%; Chistye Gazy Plus Ltd, Russia) and ultra-high-purity hydrogen (purity > 99.999%; AlfaGas Ltd, Russia) gases were used without additional purification. Hydrogen gas was enriched with the para isomer using a Bruker BPHG-90 parahydrogen generator operating at 45 K, resulting in 83% p-H_2 enrichment. The volumetric feed flow rates of hydrogen and propylene were regulated using Bronkhorst mass flow controllers; hydrogen gas flow rate was set at 180 ± 2 ml_n min^{-1}; propylene gas flow rate was set at 45 ± 1 ml_n min^{-1} to achieve the propylene:p-H_2 enriched hydrogen gas ratio of 1:4. The gases were mixed in a 500 ml stainless steel double-end cylinder and the resulting mixture was supplied to the catalyst (20 mg) placed at the bottom of a 10 mm o.d. NMR tube through a 1/16 in. o.d. (1/32 in. i.d.) PTFE capillary. In the NMR tube, the gas mixture was flowing from the bottom to the top and then to the vent through a 1/8 in. o.d. PTFE tubing connected with the NMR tube through a wye-type fitting. NMR tube with the catalyst was heated up to 130 °C using Bruker variable temperature unit. All hydrogenation experiments were performed at 2 bar; the reaction pressure was controlled using a Swagelok membrane back pressure regulator.

Hydrogenation was performed in the 7.05 T magnetic field of a 300 MHz Bruker AV 300 NMR spectrometer (PASADENA procedure [2]). A 10 mm BBO 300 MHz Bruker probe head was used. ^{1}H PASADENA NMR spectra were acquired using a $\pi/4$ rf pulse, and the spectra of a reaction mixture in thermal equilibrium were acquired using a $\pi/2$ rf pulse.

2.3 Calculations

2.3.1 Evaluation of Conversion

Propylene conversion was calculated as the molar ratio of the reaction product—propane—to the sum of propane and unreacted propylene. Catalytic reactor effluent gas was collected in an empty 10 mm o.d. NMR tube to evaluate propylene conversion over Rh/TiO_2. Conversion values were evaluated from ^{1}H NMR spectra acquired in thermal equilibrium after a complete relaxation of hyperpolarization.

2.3.2 Evaluation of Proton Polarization Losses Caused by Relaxation

To evaluate proton polarization losses caused by nuclear spin relaxation, the longitudinal relaxation times (T_1) were measured using the standard inversion-recovery pulse sequence; inverse gated ^{1}H decoupling was applied during ^{13}C NMR spectra

acquisition. It was found that proton T_1 relaxation times for the CH_2 and CH_3 groups of propane are 350 ± 20 and 345 ± 20 ms, respectively, under the reaction conditions (130 °C; 2 bar; propane:n-H_2 ratio of 1:3). Then, the time that propane molecules spent on the way from the catalyst, on the surface of which propane is formed, to the end of the detection coil region was estimated. The geometry of the NMR tube and the detection coil were described in detail previously [40, 41]. The volumetric gas flow rate u was recalculated to account for the difference in the actual and normal conditions (actual conditions: 130 °C, 2 bar; 0.25 is the mole fraction of propane at 100% conversion):

$$u = \frac{45}{60} \cdot \frac{1}{2} \cdot \frac{1}{0.25} \cdot \frac{403.15}{273.15} = 2.21 \text{ ml s}^{-1}.$$

Considering the flow rate of 2.21 ml s^{-1}, the residence time (τ_1) of propane molecules at the bottom of NMR tube below the sensitive zone with the volume V_1 estimated as 0.3 ml can be evaluated as

$$\tau_1 = \frac{V_1}{u} = \frac{0.30}{2.21} = 0.14\,s.$$

Polarization losses can be estimated based on the ratio of the averaged polarization of the molecules in the detection coil region (P_2) to the initial polarization (P_0) using the formula [41]:

$$\frac{P_2}{P_0} = \frac{uT_1}{V_2}\left(1 - e^{-\frac{V_2}{uT_1}}\right) \cdot e^{-\frac{\tau_1}{T_1}}$$

where V_2 is the volume of the sensitive region of the detection coil estimated as 1.2 ml. The ratio $\frac{P_2}{P_0}$ is ~0.34 for both propane groups under these conditions.

2.3.3 Evaluation of the Uncertainty in the ^{13}C T_1 Measurements

The uncertainty in the ^{13}C T_1 measurements was estimated from the uncertainty in the integration. For different delays after an inversion pulse (τ), the signal-to-noise ratio (SNR) for both methyl and methylene signals in ^{13}C spectra was determined and the relative standard deviation (RSD) value for the signal integrals was calculated as $\text{RSD} = \frac{86}{\text{SNR}}$ [42]. Then, the obtained relative standard deviations of the integrals were used in the experimental data approximation.

2.3.4 Reproducibility Analysis

To evaluate the reproducibility of the results, PHIP experiments were independently repeated three times, each time with a new catalyst loading. The standard deviation values were found to be 9% for conversion and 20% for proton and carbon polarization levels.

3 Results and Discussion

It is known that rhodium metal catalysts supported on titania exhibit high activity in pairwise parahydrogen addition providing higher polarization levels in HET-PHIP among other supported metal catalysts [43]. Here in this work, we used a 1 wt% Rh/TiO_2 catalyst; its preparation procedure is described in the Experimental Section. Propylene hydrogenation was performed in the high magnetic field of the NMR spectrometer under PASADENA experimental conditions [2]; the catalyst was placed at the bottom of the NMR tube so that it was located below the sensitive region of the detection coil. To ensure high catalytic activity, the NMR tube with the catalyst was heated up to 130 °C and hydrogenation reaction was performed at 2 bar. The propylene:parahydrogen-enriched H_2 ratio was set to 1:4 using mass flow controllers and the total flow rate was set at 225 ml_n min^{-1}. The mixture of gases was supplied directly to the catalyst. The PASADENA ^1H NMR spectra of the reaction mixture containing propane produced in the reaction, the unreacted propylene, and H_2 were acquired in a steady-state regime using a $\pi/4$ rf pulse. To evaluate propylene conversion, the catalytic reactor effluent gas was collected in an empty 10 mm o.d. NMR tube and ^1H NMR spectra were acquired with a $\pi/2$ rf pulse under thermal equilibrium achieved after a complete relaxation of hyperpolarization. It was found that the Rh/TiO_2 catalyst exhibits high activity in propylene hydrogenation under these reaction conditions—the conversion reached $91 \pm 8\%$ (Fig. 1). Details of the conversion evaluation are given in the Experimental Section.

In the ^1H NMR spectrum of the flowing gas (Fig. 1, red spectrum), the characteristic antiphase PHIP patterns were observed. The absorptive and the emissive parts of each PASADENA antiphase multiplet were integrated independently, and their co-added absolute values were compared with the integral (normalized by the number of contributing protons) of the corresponding multiplet at thermal equilibrium to evaluate the experimentally observed signal enhancement values (SE). Under these conditions, the Rh/TiO_2 catalyst demonstrated moderate SE levels of 33 and 52 for CH_2 and CH_3 groups of propane, respectively. To estimate the polarization levels, one needs to compare the experimentally observed SE to a maximum possible SE_{theor} in such experiment. Under our experimental conditions, the maximum ^1H signal enhancement in a PASADENA experiment numerically evaluates to

$$SE_{theor} = \frac{1}{2} \cdot \frac{4x_p - 1}{3} \cdot \frac{2\gamma\hbar B_0}{kT} = \frac{4x_p - 1}{3} \cdot 27990 \quad (1)$$

at $T = 403.15$ K, $B_0 = 7.05$ T, $\pi/4$ detection pulse for PASADENA spectrum and $\pi/2$ detection pulse for the ^1H spectrum in thermal equilibrium, where x_p is the fraction of p-H_2 in the hydrogen gas [4]. This is valid for an AX spin system, while for a larger number of magnetic nuclei in a product molecule, the maximum ^1H signal enhancement in a PASADENA experiment is reduced due to the partial cancelation of individual components of the antiphase multiplet upon further splitting by the couplings with extra protons. In the case of an A_2X_6 spin system of propane with six equivalent protons in two methyl groups and two equivalent protons in the methylene group, the maximum ^1H signal enhancement that can be produced in a PASADENA

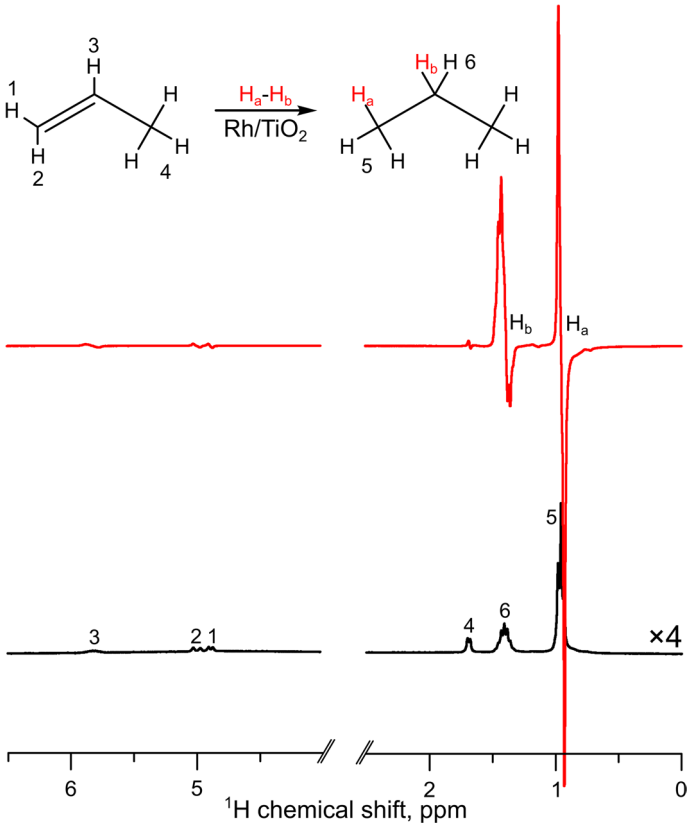

Fig. 1 Top: the reaction scheme of pairwise addition of p-H_2 to propylene over Rh/TiO_2 catalyst. Bottom: ^{1}H NMR spectrum acquired during propylene hydrogenation with p-H_2 over Rh/TiO_2 catalyst, while the gas was flowing with the flow rate of 225 ml_n min^{-1} (red spectrum), and ^{1}H NMR spectrum of the catalytic reactor effluent gas collected in an empty 10 mm o.d. NMR tube (black spectrum, intensity is multiplied by a factor of 4). The ^{1}H PASADENA spectrum was acquired using a $\pi/4$ rf pulse; the corresponding ^{1}H spectrum in thermal equilibrium was acquired using a $\pi/2$ rf pulse (Color figure online)

experiment reduces differently for the CH_2 and CH_3 groups. The pattern of line intensities for the CH_2 group coupled to six equivalent protons in a ^{1}H NMR spectrum is (1,6,15,20,15,6,1) for thermally polarized propane and $(1,4,5,0,-5,-4,-1)$ for the PASADENA experiment [44]. In the case of a CH_3 group coupled to two equivalent protons, the pattern of line intensities is (1,2,1) under thermal equilibrium and $(1,0,-1)$ for the PASADENA experiment. Therefore, the maximum possible ^{1}H signal enhancement is reduced by factors of 3.2 and 2 for the CH_2 and the CH_3 group, respectively (both the emissive and the absorptive parts of the antiphase multiplet are taken into account). Moreover, it should be noted that the maximum possible ^{1}H SE_{theor} in a PASADENA experiment significantly depends on the line broadening because of a partial signal cancellation of the overlapping absorption and emission parts of the antiphase multiplet. The simulation of the experimental ^{1}H

PASADENA spectrum was performed to determine the width of individual lines in the experimental spectra. The maximum possible ^{1}H SE_{theor} value was determined from the simulated spectra of both hyperpolarized and thermally polarized propane with the corresponding line width. At $x_p = 83\%$ parahydrogen enrichment level, the maximum ^{1}H signal enhancement for the CH_2 and the CH_3 groups of propane is 5440 and 8500, respectively. Therefore, the estimated proton polarization was $0.6 \pm 0.1\%$ for both groups under these reaction conditions.

The ^{1}H polarization levels estimated above are the lower estimates, since the relaxation losses were not taken into account. To evaluate polarization losses caused by nuclear spin relaxation, the longitudinal relaxation times for both CH_2 and CH_3 groups of propane were measured under reaction conditions (130 °C, 2 bar). To that end, propane and normal hydrogen (n-H_2) gases were supplied with a 1:3 ratio (as if propylene completely converted to propane; the propane:n-H_2 ratio was set using mass flow controllers) to the bottom of an empty 10 mm o.d. NMR tube. The NMR tube was heated up to 130 °C, and the ^{1}H T_1 measurements were performed at 2 bar for a static gas. It was found that proton T_1 relaxation times for the CH_2 and CH_3 groups of propane are 350 ± 20 and 345 ± 20 ms, respectively. The estimates provided in the Experimental Section demonstrate that only one-third of the initial polarization is observed and that the initial ^{1}H polarization levels are thus ~ $1.8 \pm 0.4\%$.

To examine the possibility of polarization transfer from ^{1}H to ^{13}C nuclei in the gas phase, the application of an rf pulse sequence seems the best choice, since longitudinal T_1 relaxation times for both ^{1}H and ^{13}C nuclei of propane in the gas phase are short. This makes the alternative approach based on magnetic field cycling ineffective in this case, because it requires multi-second-long sample manipulation time period, during which the produced ^{13}C hyperpolarized state would decay. The proton T_1 relaxation time for propane in propane/H_2 mixtures increases nearly linearly with propane mole fraction and pressure [45, 46], indicating that propane T_1 relaxation in the gas phase is mostly governed by the spin-rotation interaction [47]. As stated above, the T_1 times for propane protons under reaction conditions are ~ 350 ms. For ^{13}C nuclei in propane, we found that ^{13}C T_1 relaxation times for the methylene ($^{13}CH_2$) and methyl ($^{13}CH_3$) groups are 140 ± 10 and 149 ± 8 ms for propane mixed with hydrogen gas in the 1:3 molar ratio at room temperature, and even shorter values can be expected at 130 °C [37]. The T_1 relaxation times being shorter for heteronuclei compared to ^{1}H nuclei is a common situation in the NMR of gases [48, 49]; it is attributed to the predominance of the spin-rotation relaxation mechanism for molecular gases and vapors and is associated with the properties of the spin-rotation tensor for a specific nucleus.

It is important to note that propylene gas used in the hydrogenation experiments was not isotopically labeled. Taking into account the natural abundance of ^{13}C nuclei, it is assumed that the mole fraction of [1-^{13}C]propane is 2.2% (positions #1 and #3 are identical in thermal equilibrium, Fig. 2) and the fraction of [2-^{13}C] propane is 1.1%. The molecules containing two ^{13}C nuclei were not considered due to vanishingly low probabilities. Therefore, ^{13}C NMR spectrum of propane in thermal equilibrium is the superposition of the signals from two different isotopomers—[1-^{13}C]propane and [2-^{13}C]propane (see ^{13}C spectra in Fig. 2). It can be seen from

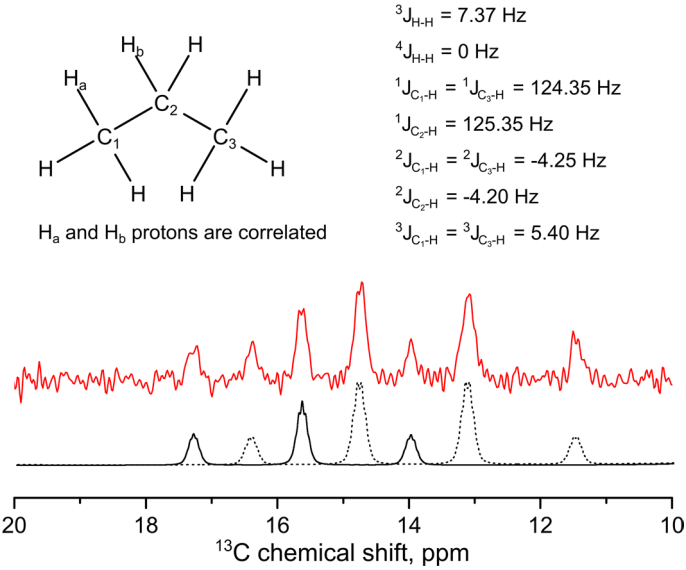

Fig. 2 Top: propane J-couplings. Most of the coupling constants were taken from the literature [50]. The corrected $^{2}J_{C_2-H}$ and $^{3}J_{C_1-H}$ coupling constant values were obtained from the experimental ^{13}C NMR spectrum of thermally polarized propane (saturated solution in acetone-d_6). Bottom: an experimental ^{13}C NMR spectrum of thermally polarized propane in the gas phase (red line). Simulated spectra of [2-^{13}C] propane (solid black line) and [1-^{13}C]propane (dashed black line) are shown below (Color figure online)

Fig. 2 that the experimental and simulated ^{13}C NMR spectra of propane gas in thermal equilibrium are in a good agreement. However, the incorporation of p-H_2-derived protons in a molecule (denoted as H_a and H_b in Fig. 2) makes carbons #1 and #3 non-identical, so in the case of PHIP, three different isotopomers—[1-^{13}C]propane, [2-^{13}C]propane and [3-^{13}C]propane—should be considered.

The PH-INEPT pulse sequence was chosen for the experiments aiming to transfer the parahydrogen-derived polarization from ^{1}H to ^{13}C nuclei in the gas phase as one of the most robust and effective approaches. However, the performance of INEPT-based polarization transfer schemes strongly depends on the precise choice of the inter-pulse delays. The optimal delay values are determined by the network of scalar couplings in the molecule and in some simple cases they can be derived analytically [33], but numerical calculations are more appropriate when analyzing complex molecules with a large number of spins. Here, we simulated the spectra expected after the application of PH-INEPT and PH-INEPT + sequences utilizing the approach described earlier [51]. We have considered the full spin system of propane, including eight protons and one ^{13}C nucleus. In the initial spin density matrix, one proton from the CH_3 group and one proton from the CH_2 group are in the singlet spin state, while other nuclei are not polarized. To take into account the rapid decay of coherences occurring in the course of the reaction, the non-diagonal terms of the initial spin density matrix were omitted, which is a common procedure. Thus, the initial spin order corresponds to $\widehat{I}_{1z}\widehat{I}_{2z}$ operator (neglecting the unity matrix), where $\widehat{I}_{1,2}$ are spin operators of the p-H_2-derived protons in the propane molecule.

This density matrix was then subjected to a set of rotations and periods of free evolution under Zeeman and J-coupling interactions corresponding to PH-INEPT and PH-INEPT + pulse sequences. The schemes of corresponding experiments are depicted in Figs. 3a and 5a. In the case of PH-INEPT, we assessed the efficiency of polarization transfer by calculating the expectation value for transverse magnetization of heteronucleus being antiphase with respect to the p-H_2-derived protons. To do this, the trace of the product of the final density matrix and the sum of antiphase product operators $2\widehat{I}_{1z}\widehat{S}_y$ and $2\widehat{I}_{2z}\widehat{S}_y$ was taken, where $\widehat{S}$ is the spin operator of ^{13}C nucleus. It should be noted that, while in the experimental NMR spectra exhibiting antiphase signals their broadening causes partial overlap of the signals of opposite sign and thus a reduction in signal intensity, these effects are not present in the theoretical treatment of the performance of pulse sequences which evaluates spin density matrix elements. In the PH-INEPT + sequence, additional refocusing allows one to produce net magnetization of a heteronucleus. Thus, to determine the efficiency of transfer by PH-INEPT + we calculated the trace of the product of the final density matrix and the $\widehat{S}_x$ operator. The fact that ^{1}H polarization levels achieved in the HET-PHIP experiment are not 100% is immaterial and was not taken into account in the polarization transfer efficiency calculations.

The PH-INEPT sequence has only one parameter to optimize: the inter-pulse delay τ_1; the results of numerical simulation of the ^{13}C polarization achieved by PH-INEPT as a function of delay τ_1 are presented in Fig. 3b for three different propane isotopomers. It is found that for both [1-^{13}C]propane and [2-^{13}C]propane the optimal τ_1 delay is 14.0 ms; at this delay time the efficiency of p-H_2-derived polarization transfer to ^{13}C nucleus in [1-^{13}C]propane and [2-^{13}C]propane isotopomers using PH-INEPT is estimated as ~ 14%. In the case of [3-^{13}C]propane the efficiency of the polarization transfer using PH-INEPT is lower (green spectrum in Fig. 3c) due to small J-coupling constants between the p-H_2-derived protons and the ^{13}C nucleus (Fig. 2). It should be noted that PH-INEPT pulse sequence does not transfer any proton magnetization of thermally polarized propane isotopomers [33]; thus, only the molecules with p-H_2-derived protons contribute to ^{13}C PH-INEPT spectrum provided that the thermal equilibrium ^{13}C NMR signal can be neglected. The efficiency of the PH-INEPT sequence primarily depends on the value of the mutual spin–spin coupling constant of the two p-H_2-derived protons ($H_a - H_b$) and their couplings to the ^{13}C nucleus ($H_{a(b)}$–^{13}C). In propane these couplings are large; however, coupling to additional nuclei in the 9-spin system of propane isotopomers causes a significant signal reduction.

The PH-INEPT pulse sequence with a 14.0 ms delay τ_1 was applied, while propylene:parahydrogen-enriched H_2 gas mixture was supplied to the catalyst and ^{1}H HP propane was constantly formed at the bottom of the NMR tube and was then flowing upward in the NMR tube through the sensitive region of the detection coil. An experimental ^{13}C NMR spectrum acquired after ^{13}C hyperpolarization of propane isotopomers using PH-INEPT pulse sequence is presented in Fig. 3c (red spectrum). Two multiplets are observed in the spectrum—a quartet with a $(-1,-1,1,1)$ lines pattern at 13.87 ppm attributed to the methyl group of [1-^{13}C] propane, and a triplet with a $(-1,0,1)$ pattern at 15.26 ppm attributed to the methylene group of [2-^{13}C]propane. Moreover, the ^{13}C NMR spectra were simulated for

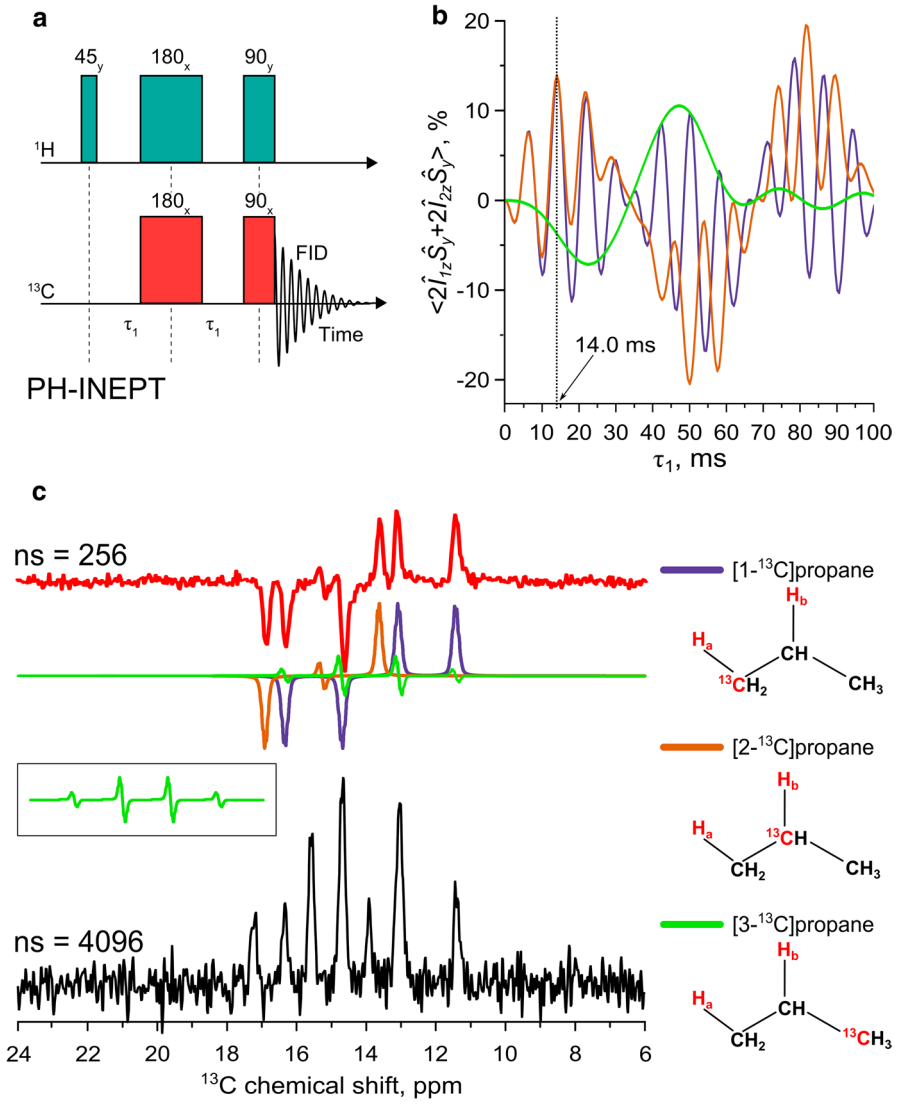

Fig. 3 **a** PH-INEPT pulse sequence used to transfer polarization from ^{1}H-to-^{13}C nuclei in propane. **b** Numerical simulation of the ^{13}C polarization transferred by PH-INEPT for three different propane isotopomers as a function of delay τ_1. **c** Experimental ^{13}C NMR spectrum acquired after ^{13}C hyperpolarization of propane isotopomers using PH-INEPT pulse sequence (red spectrum; the optimal delay τ_1 of 14.0 ms was used; 256 accumulations) during propylene hydrogenation with p-H_2 and simulated spectra presented separately for the three different isotopomers (the scaled spectrum for [3-^{13}C]propane is presented in the inset). The experimental ^{13}C NMR spectrum of pure thermally polarized propane (black spectrum; 4096 accumulations) is presented below

all three propane isotopomers, demonstrating a good agreement with the experiment (Fig. 3c). It is interesting to note that for ^{13}C HP [3-^{13}C]propane all lines of the quartet are antiphase (green spectrum in Fig. 3c), meaning that [3-^{13}C]propane

molecules do not contribute to the line integrals used in the evaluation of ^{13}C NMR signal enhancement.

To evaluate ^{13}C SE values, a ^{13}C NMR spectrum of pure propane in thermal equilibrium and 1 atm was acquired. ^{13}C SE values were calculated as the ratio of the sum of absolute integrals of the polarized multiplets to the integral in ^{13}C spectrum at thermal equilibrium, with the difference in the number of signal accumulations, the total pressure, and the gas mixture composition taken into account. It was found that the experimentally observed signal enhancement values are 29 and 13 for the methyl group of [1-^{13}C]propane and the methylene group of [2-^{13}C]propane, respectively. The effect of the splitting of an antiphase multiplet due to the coupling to several equivalent nuclei should be taken into account for ^{13}C polarization calculations, similar to the ^{1}H case described above. The pattern of line intensities for the ^{13}C nucleus coupled to three equivalent protons in the methyl group is $(-1,-1,1,1)$ in the case of hyperpolarization and (1,3,3,1) in thermal equilibrium. The ^{13}C nucleus coupled to two equivalent protons in the methylene group gives a $(-1,0,1)$ pattern in the case of hyperpolarization and a (1,2,1) pattern in thermal equilibrium. This means that the maximum achievable ^{13}C signal enhancement is reduced by a factor of 2 for both $^{13}CH_2$ and $^{13}CH_3$ groups. The maximum possible ^{13}C signal enhancement under PASADENA condition is ~ 3.977 times higher than in Eq. (1) due to the difference in the gyromagnetic ratios for ^{13}C and ^{1}H nuclei, and taking into account the effect of signal splitting the maximum ^{13}C SE_{theor} is 43030 at $x_p = 83\%$ parahydrogen enrichment level. Therefore, ^{13}C polarization is estimated as $0.07 \pm 0.01\%$ and $0.030 \pm 0.006\%$ for the methyl group of [1-^{13}C]propane and the methylene group of [2-^{13}C]propane, respectively.

The τ_1 delays in the experiments with PH-INEPT pulse sequence were also varied. Experimental ^{13}C NMR spectra acquired after ^{1}H-to-^{13}C hyperpolarization transfer in propane isotopomers using the PH-INEPT pulse sequence with different τ_1 delays are shown in Fig. 4b along with the corresponding simulated spectra presented separately for three different isotopomers. The experimental dependence of ^{13}C polarization for the methyl group of [1-^{13}C]propane (purple circles in Fig. 4a) and for the methylene group of [2-^{13}C]propane (orange diamonds in Fig. 4a) on the inter-pulse delay τ_1 is well fitted by the numerically simulated function; the positions of all extremes are consistent with the calculations. The significantly lower experimentally observed ^{13}C polarization compared to the calculated ones are primarily due to the moderate initial proton polarization. The second reason why the experimental ^{13}C polarization values are reduced is the ^{13}C spin relaxation, and possibly not so much T_1 as T_2 during the duration of the sequence. As can be seen, the oscillations in the τ_1-dependence are strongly damped for the experimentally observed ^{13}C polarization of the methylene group (the ^{13}C polarization for $^{13}CH_2$ group at $\tau_1 = 23.0$ ms is close to zero, Fig. 4a). This is most likely associated with a lower value of T_2 for the methylene ($^{13}CH_2$) group compared to methyl ($^{13}CH_3$), since ^{13}C T_1 relaxation times for methylene and methyl groups are similar (140 ± 10 and 149 ± 8 ms). The experimental dependence of ^{13}C polarization on τ_1 also demonstrates that the precise calculations for PH-INEPT pulse sequence are needed—even a 1 ms variation in the τ_1 delay is relevant.

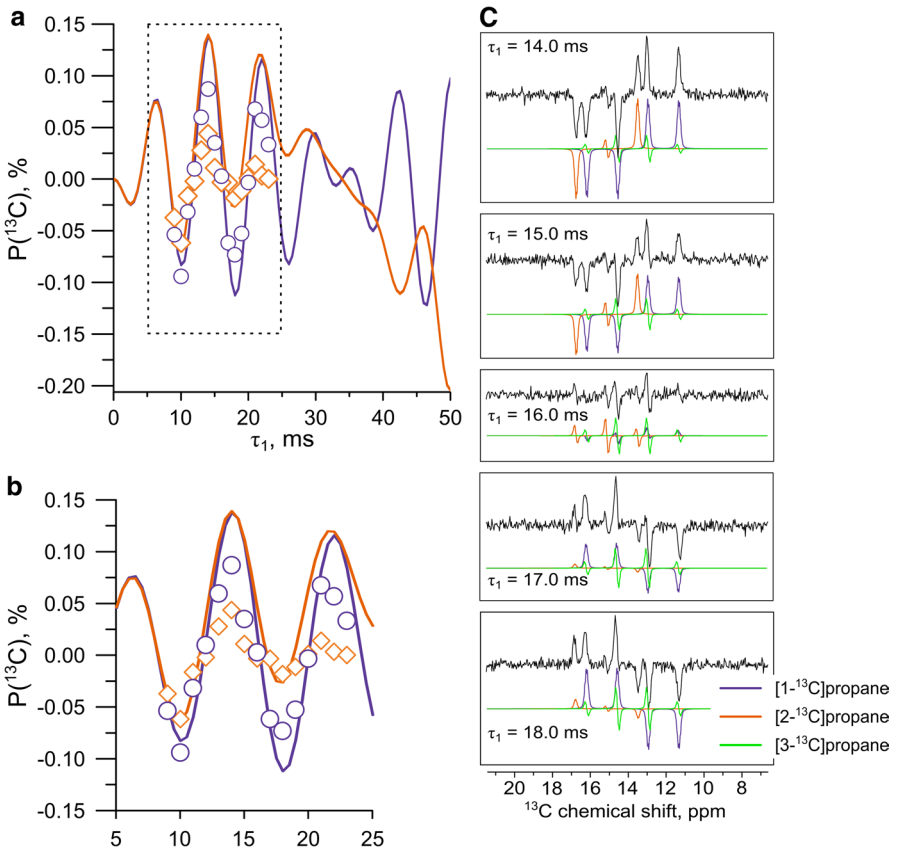

Fig. 4 **a** Experimental dependence of ^{13}C polarization for [1-^{13}C]propane and [2-^{13}C]propane (purple circles and orange diamonds, respectively) on delay τ_1 in the 9.0–23.0 ms range and the results of corresponding theoretical calculations (solid lines). Part of the graph enclosed in dashed rectangle is shown expanded in **b** to better demonstrate that experimental extremes and polarization sign changes are in a good agreement with the simulation (rescaled). **c** Experimental ^{13}C NMR spectra acquired after ^{13}C hyperpolarization of propane isotopomers using the PH-INEPT pulse sequence with different τ_1 delays, and the corresponding simulated spectra presented separately for the three different isotopomers

In addition, the PH-INEPT + pulse sequence was applied under the same experimental conditions. The antiphase signals of the PH-INEPT sequence can be refocused by employing the additional 180° pulses with a τ_2 delay on both sides (Fig. 5a). Then, the in-phase ^{13}C NMR signals obtained with PH-INEPT + can be proton-decoupled. Numerical simulations of the efficiency of the PH-INEPT + pulse sequence were performed for all propane isotopomers. The τ_1 delay was set to 14.0 ms; the ^{13}C polarization provided by PH-INEPT + for three different propane isotopomers as a function of delay τ_2 is presented in Fig. 5b. It was found that for $\tau_2 = 3.0$ ms, [1-^{13}C]propane and [2-^{13}C]propane demonstrate the polarization of opposite signs. An experimental ^{13}C{^{1}H} NMR spectrum acquired after the ^{1}H-to-^{13}C hyperpolarization transfer in the propane

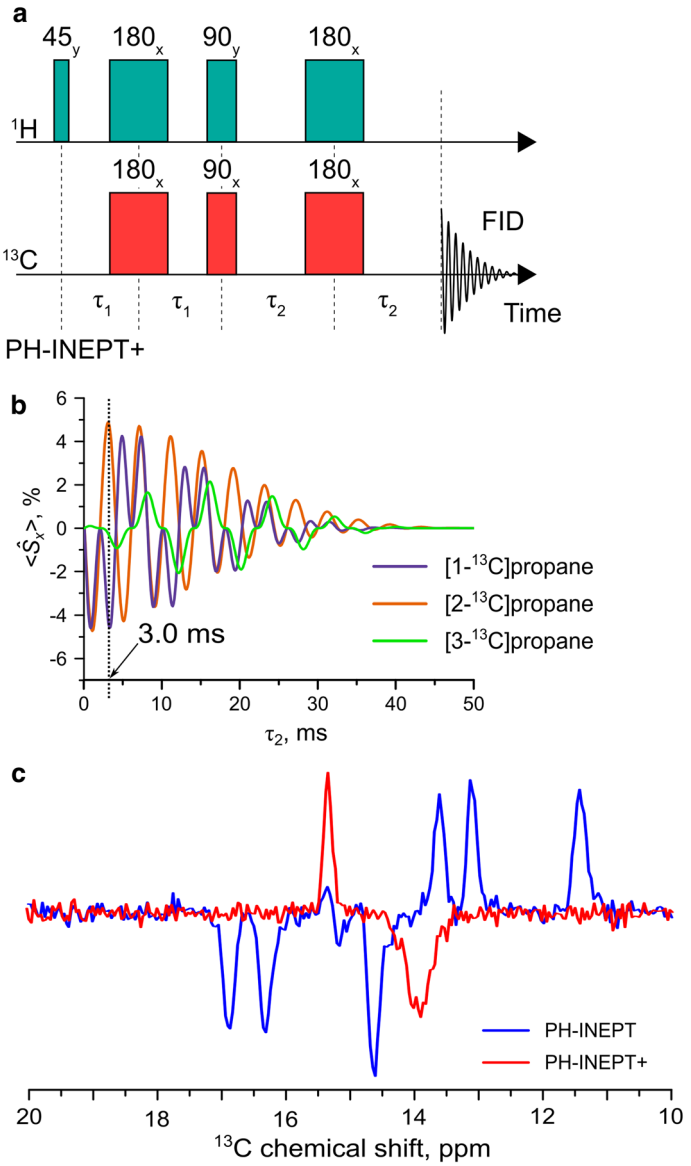

Fig. 5 **a** PH-INEPT + pulse sequence used to transfer polarization from ^{1}H to ^{13}C in propane. **b** Numerical simulation of the ^{13}C polarization as a function of delay τ_2 presented for all three propane isotopomers. For numerical calculation delay τ_1 was set at 14.0 ms as the optimal delay for PH-INEPT. **c** Experimental ^{13}C NMR spectrum acquired after the ^{1}H-to-^{13}C hyperpolarization transfer in the propane isotopomers using the PH-INEPT + pulse sequence (red spectrum; the optimal delay τ_1 of 14.0 ms and τ_2 of 3.0 ms was used; proton decoupling was used during ^{13}C signal acquisition) during propylene hydrogenation with p-H_2 and the spectrum of ^{13}C hyperpolarized propane via PH-INEPT (blue spectrum; τ_1 of 14.0 ms was used). Both spectra are presented on the same vertical scale

isotopomers using PH-INEPT + pulse sequence ($\tau_1 = 14.0$ ms, $\tau_2 = 3.0$ ms) is presented in Fig. 5c (red spectrum). This spectrum exhibits only two signals of opposite signs at the chemical shifts of the corresponding multiplets, as expected. The ^{13}C NMR signal enhancement is 13 and 7 for the methyl group of [1-^{13}C]propane and the methylene group of [2-^{13}C]propane, respectively. These SE values correspond to the ^{13}C polarization of 0.029 and 0.015%, which are about 2.5 times lower compared to those obtained with PH-INEPT; this observation is also consistent with the numerical calculations (polarization efficiency of 14% and 5% in the case of the PH-INEPT and the PH-INEPT + sequence, respectively). The fact that theoretically calculated efficiency of PH-INEPT + sequence is measurably lower than that of PH-INEPT indicates that additional protons in the spin system interfere strongly with the complete refocusing of ^{13}C antiphase magnetization by the PH-INEPT + sequence. Moreover, the refocusing step requires an additional delay of $2\tau_2 = 6.0$ ms, which in the experimental spectra leads to further polarization losses due to rapid T_2 relaxation. All these effects surpass the positive effect of alleviated partial cancellation for antiphase signals, thus demonstrating the suboptimal performance of PH-INEPT + in the case of propane.

4 Conclusions

Here, in this work, we examined the possibility of the polarization transfer from ^{1}H to ^{13}C nuclei in the gas phase using PH-INEPT-based sequences. Proton hyperpolarization was produced via parahydrogen-induced polarization method using a heterogeneous hydrogenation catalyst. Natural abundance propylene was hydrogenated with p-H_2 over 1 wt% Rh/TiO_2 catalyst under PASADENA experimental conditions. The apparent proton polarization was estimated as 1.8 ± 0.4%, taking into account the polarization losses caused by spin relaxation. PH-INEPT and PH-INEPT + pulse sequences were examined in this work. The optimal interpulse delays for both PH-INEPT and PH-INEPT + sequences were determined via numerical calculations for the full spin system of propane that includes eight protons and one ^{13}C nucleus. All three propane ^{13}C isotopomers were considered. The application of an optimized PH-INEPT polarization transfer sequence resulted in the ^{13}C polarization values of 0.07 ± 0.01% and 0.030 ± 0.006% for the methyl group of [1-^{13}C]propane and the methylene group of [2-^{13}C]propane, respectively. The experimental dependence of ^{13}C polarization values for [1-^{13}C]propane and [2-^{13}C]propane on the PH-INEPT delay τ_1 is in a good agreement with the simulation. The resulting ^{13}C polarization using PH-INEPT + sequence is ~ 2.5 times lower, which is also consistent with the numerical calculations.

Acknowledgements VPK thanks Prof. Konstantin L. Ivanov, deceased on March 5, 2021 at the age of 44, for the expert guidance in his mastering the spin dynamics calculations. All authors acknowledge Prof. Konstantin L. Ivanov and Dr. Kirill V. Kovtunov who initiated this work and made a major contribution to the field of hyperpolarized NMR.

Author Contributions Conceptualization: KVK; supervision: OGS, KVK, IVK, EYC; resources—catalyst: LMK, VIB; investigation—DBB, VPK, OGS, SVS; writing–original draft preparation: DBB, VPK, SVS; writing–review and editing: OGS, IVK, EYC. The manuscript was reviewed by all authors.

Funding The HET-PHIP experiments performed by DBB, SVS, OGS, and IVK were funded by Russian Foundation for Basic Research (RFBR; Grants no. 19-29-10003 and 19-33-60045). The spin dynamics calculation performed by VPK was supported by RFBR grant no. 19-29-10028. The catalyst preparation performed by LMK was supported by the Ministry of Science and Higher Education of the Russian Federation (project # AAAA-A21-121011390011-4). EYC thanks the following for funding support: DOD CDMRP W81XWH15-1-0271 and W81XWH-20-10576, National Heart, Lung, and Blood Institute 1 R21 HL154032-01 and NSF CHE-1904780.

Declarations

Conflict of Interest EYC declares a stake of ownership in XeUS Technologies LTD.

References

1. R.A. Green, R.W. Adams, S.B. Duckett, R.E. Mewis, D.C. Williamson, G.G.R. Green, Prog. Nucl. Magn. Reson. Spectrosc. **67**, 1 (2012)
2. C.R. Bowers, D.P. Weitekamp, J. Am. Chem. Soc. **109**, 5541 (1987)
3. M.G. Pravica, D.P. Weitekamp, Chem. Phys. Lett. **145**, 255 (1988)
4. C.R. Bowers, in *Encycl. Magn. Reson.*, ed. by R.K. Harris, R. Wasylishen (John Wiley, Chichester, 2007), p. 750. https://doi.org/10.1002/9780470034590.emrstm0489
5. A. Eichhorn, A. Koch, J. Bargon, J. Mol. Catal. A Chem. **174**, 293 (2001)
6. L.-S. Bouchard, S.R. Burt, M.S. Anwar, K.V. Kovtunov, I.V. Koptyug, A. Pines, Science **319**, 442 (2008)
7. K.V. Kovtunov, I.E. Beck, V.I. Bukhtiyarov, I.V. Koptyug, Angew. Chem. Int. Ed. **47**, 1492 (2008)
8. K.V. Kovtunov, O.G. Salnikov, I.V. Skovpin, N.V. Chukanov, D.B. Burueva, I.V. Koptyug, Pure Appl. Chem. **92**, 1029 (2020)
9. E.V. Pokochueva, D.B. Burueva, O.G. Salnikov, I.V. Koptyug, ChemPhysChem (2021). https://doi.org/10.1002/cphc.202100153
10. A. Kopanski, F. Hane, T. Li, M. Albert, in *25th ISMRM Conf.* (Honolulu, HI, USA, 2017), p. 2162
11. K.V. Kovtunov, I.V. Koptyug, M. Fekete, S.B. Duckett, T. Theis, B. Joalland, E.Y. Chekmenev, Angew. Chem. Int. Ed. **59**, 17788 (2020)
12. K.V. Kovtunov, M.L. Truong, D.A. Barskiy, I.V. Koptyug, A.M. Coffey, K.W. Waddell, E.Y. Chekmenev, Chem. A Eur. J. **20**, 14629 (2014)
13. O.G. Salnikov, P. Nikolaou, N.M. Ariyasingha, K.V. Kovtunov, I.V. Koptyug, E.Y. Chekmenev, Anal. Chem. **91**, 4741 (2019)
14. O.G. Salnikov, K.V. Kovtunov, P. Nikolaou, L.M. Kovtunova, V.I. Bukhtiyarov, I.V. Koptyug, E.Y. Chekmenev, ChemPhysChem **19**, 2621 (2018)
15. Y. Du, R. Behera, R.V. Maligal-Ganesh, M. Chen, E.Y. Chekmenev, W. Huang, C.R. Bowers, J. Phys. Chem. C **124**, 8304 (2020)
16. O.G. Salnikov, A. Svyatova, L.M. Kovtunova, N.V. Chukanov, V.I. Bukhtiyarov, K.V. Kovtunov, E.Y. Chekmenev, I.V. Koptyug, Chem. A Eur. J. **27**, 1316 (2021)
17. L.T. Kuhn, J. Bargon, in *Situ NMR Methods Catal.*, ed. by J. Bargon, L.T. Kuhn (Springer, Berlin, Heidelberg, 2006), p. 25. https://doi.org/10.1007/128_064
18. F. Reineri, E. Cavallari, C. Carrera, S. Aime, Magn. Reson. Mater. Phys. Biol. Med. **34**, 25 (2021)
19. S. Siddiqui, S. Kadlecek, M. Pourfathi, Y. Xin, W. Mannherz, H. Hamedani, N. Drachman, K. Ruppert, J. Clapp, R. Rizi, Adv. Drug Deliv. Rev. **113**, 3 (2017)
20. B. Joalland, A.B. Schmidt, M.S.H. Kabir, N.V. Chukanov, K.V. Kovtunov, I.V. Koptyug, J. Hennig, J.-B. Hövener, E.Y. Chekmenev, Anal. Chem. **92**, 1340 (2020)
21. H. Jóhannesson, O. Axelsson, M. Karlsson, Comptes Rendus Phys. **5**, 315 (2004)
22. E. Cavallari, C. Carrera, M. Sorge, G. Bonne, A. Muchir, S. Aime, F. Reineri, Sci. Rep. **8**, 8366 (2018)

23. S. Knecht, J.W. Blanchard, D. Barskiy, E. Cavallari, L. Dagys, E. van Dyke, M. Tsukanov, B. Bliemel, K. Münnemann, S. Aime, F. Reineri, M.H. Levitt, G. Buntkowsky, A. Pines, P. Blümler, D. Budker, J. Eills, Proc. Natl. Acad. Sci. **118**, e2025383118 (2021)
24. A.N. Pravdivtsev, A.V. Yurkovskaya, H.-M. Vieth, K.L. Ivanov, J. Chem. Phys. **139**, 244201 (2013)
25. A.S. Kiryutin, A.N. Pravdivtsev, K.L. Ivanov, Y.A. Grishin, H.-M. Vieth, A.V. Yurkovskaya, J. Magn. Reson. **263**, 79 (2016)
26. K. Golman, O. Axelsson, H. Jóhannesson, S. Månsson, C. Olofsson, J.S.S. Petersson, Magn. Reson. Med. **46**, 1 (2001)
27. M. Goldman, H. Jóhannesson, O. Axelsson, M. Karlsson, Magn. Reson. Imaging **23**, 153 (2005)
28. M. Roth, A. Koch, P. Kindervater, J. Bargon, H.W. Spiess, K. Münnemann, J. Magn. Reson. **204**, 50 (2010)
29. G. Stevanato, J. Eills, C. Bengs, G. Pileio, J. Magn. Reson. **277**, 169 (2017)
30. G. Stevanato, J. Magn. Reson. **274**, 148 (2017)
31. S. Bär, T. Lange, D. Leibfritz, J. Hennig, D. von Elverfeldt, J.-B. Hövener, J. Magn. Reson. **225**, 25 (2012)
32. A.N. Pravdivtsev, A.V. Yurkovskaya, N.N. Lukzen, K.L. Ivanov, H.-M. Vieth, J. Phys. Chem. Lett. **5**, 3421 (2014)
33. M. Haake, J. Natterer, J. Bargon, J. Am. Chem. Soc. **118**, 8688 (1996)
34. M. Goldman, H. Jóhannesson, Comptes Rendus Phys. **6**, 575 (2005)
35. S. Kadlecek, K. Emami, M. Ishii, R. Rizi, J. Magn. Reson. **205**, 9 (2010)
36. C. Cai, A.M. Coffey, R.V. Shchepin, E.Y. Chekmenev, K.W. Waddell, J. Phys. Chem. B **117**, 1219 (2013)
37. C.J. Jameson, in *Gas phase NMR*. ed. by K. Jackowski, M. Jaszuński (The Royal Society of Chemistry, Cambridge, 2016), p. 1
38. K. Jackowski, M. Jaszuński, Concepts Magn. Reson. Part A **30A**, 246 (2007)
39. E.V. Pokochueva, D.B. Burueva, L. Kovtunova, A.V. Bukhtiyarov, A.Y. Gladky, K.V. Kovtunov, I.V. Koptyug, V.I. Bukhtiyarov, Faraday Discuss. **229**, 161 (2021)
40. D.A. Barskiy, O.G. Salnikov, K.V. Kovtunov, I.V. Koptyug, J. Phys. Chem. A **119**, 996 (2015)
41. O.G. Salnikov, L.M. Kovtunova, I.V. Skovpin, V.I. Bukhtiyarov, K.V. Kovtunov, I.V. Koptyug, ChemCatChem **10**, 1178 (2018)
42. P.A. Hays, T. Schoenberger, Anal. Bioanal. Chem. **406**, 7397 (2014)
43. K.V. Kovtunov, D.A. Barskiy, A.M. Coffey, M.L. Truong, O.G. Salnikov, A.K. Khudorozhkov, E.A. Inozemtseva, I.P. Prosvirin, V.I. Bukhtiyarov, K.W. Waddell, E.Y. Chekmenev, I.V. Koptyug, Chem. A Eur. J. **20**, 11636 (2014)
44. K.V. Kovtunov, I.V. Koptyug, in *Magn. Reson. Microsc. Spat. Resolv. NMR Tech. Appl.*, ed. by S.L. Codd, J.D. Seymour (Wiley-VCH, Weinheim, 2008), p. 99. https://doi.org/10.1002/9783527626052.ch7
45. D.A. Barskiy, K.V. Kovtunov, E.Y. Gerasimov, M.A. Phipps, O.G. Salnikov, A.M. Coffey, L.M. Kovtunova, I.P. Prosvirin, V.I. Bukhtiyarov, I.V. Koptyug, E.Y. Chekmenev, J. Phys. Chem. C **121**, 10038 (2017)
46. N.M. Ariyasingha, O.G. Salnikov, K.V. Kovtunov, L.M. Kovtunova, V.I. Bukhtiyarov, B.M. Goodson, M.S. Rosen, I.V. Koptyug, J.G. Gelovani, E.Y. Chekmenev, J. Phys. Chem. C **123**, 11734 (2019)
47. R.E.D. McClung, in *Encycl. Magn. Reson.*, ed. by R.K. Harris, R.L. Wasylishen (John Wiley, Chichester, 2007), p. 1. https://doi.org/10.1002/9780470034590.emrstm0524
48. C.J. Jameson, A.K. Jameson, N.C. Smith, J.K. Hwang, T. Zia, J. Phys. Chem. **95**, 1092 (1991)
49. M.M. Folkendt, B.E. Weiss-Lopez, N.S. True, J. Phys. Chem. **92**, 4859 (1988)
50. R.E. Wasylishen, T. Schaefer, Can. J. Chem. **52**, 3247 (1974)
51. A. Svyatova, V.P. Kozinenko, N.V. Chukanov, D.B. Burueva, E.Y. Chekmenev, Y.W. Chen, D.W. Hwang, K.V. Kovtunov, I.V. Koptyug, Sci. Rep. **11**, 5646 (2021)